J. Fluid Mech. (1969), *vol.* 37, *part* 1, *pp.* 95–114
Printed in Great Britain

Calculation of incompressible flow past a circular cylinder at moderate Reynolds numbers

By ROBERT LEIGH UNDERWOOD†
Department of Aeronautics and Astronautics, Stanford University

(Received 14 October 1968)

The steady, two-dimensional, incompressible flow past a circular cylinder is calculated for Reynolds numbers up to ten. An accurate description of the flow field is found by employing the semi-analytical method of series truncation to reduce the governing partial differential equations of motion to a system of ordinary differential equations which can be integrated numerically. Results are given for Reynolds numbers between 0·4 and 10·0 (based on diameter). The Reynolds number at which separation first occurs behind the cylinder is found to be 5·75. Over the entire Reynolds number range investigated, characteristic flow parameters such as the drag coefficient, pressure coefficient, standing eddy length, and streamline pattern compare favourably with available experimental data and numerical solution results.

1. Introduction

For more than a century, the circular cylinder has held a prominent place in the study of viscous, incompressible flow at low and moderate Reynolds numbers (i.e. Reynolds numbers of order 10 or smaller). The first theoretical treatment of the problem was given by Stokes, who could find no steady flow satisfying his linearized governing equations. This was the famous Stokes' paradox; and it remained unresolved until Oseen explained that the failure resulted from neglect of the non-linear inertia terms, which become dominant far from the body. Hence, as a remedy he suggested alternative linearized equations that partially account for the inertia terms. Soon thereafter, Lamb (1911) gave a solution of Oseen's equations for the circular cylinder which employed an approximate boundary condition at the body surface. This work was extended by Tomotika & Aoi (1950), who obtained solutions to the full Oseen equations for arbitrary Reynolds number; however, Yamada (1954) pointed out serious numerical inaccuracies in these solutions.

The solutions to Oseen's equations present a uniformly valid first approximation to the flow about a circular cylinder at low Reynolds number. Independently and nearly simultaneously, Kaplun (1957) and Proudman & Pearson (1957) generated a procedure to calculate higher approximations by matching two

† Now at Lockheed Missiles and Space Company, Sunnyvale, California.

asymptotic expansions valid, respectively, near to and far from the body. The results, though, are of limited utility for all except very small Reynolds numbers.

'Intermediately small' Reynolds numbers are those beyond the range of validity of the above approximations, but still smaller than those for which the viscous forces are in some sense negligible. For such Reynolds numbers analytical work has met extreme difficulty, so that knowledge of the resultant flows has been obtained almost exclusively either by experiment or by numerical integration of the complete governing equations of motion. Various experimental measurements of the drag coefficient at moderate Reynolds number have been made, those of Tritton (1959) having been the most extensive and careful. Another set of valuable experiments was performed by Taneda (1956), who photographed the flow past cylinders at moderate Reynolds numbers, thereby observing the Reynolds number above which separation occurs and the length of the standing vortices behind the cylinder for larger Reynolds numbers.

Previous numerical solutions of the full Navier–Stokes equations for specific low and moderate Reynolds numbers include solutions for Reynolds numbers $R = 10$ and 20 (based on diameter) by Thom (1933), for $R = 40$ by Kawaguti (1953), for $R = 40$ and 44 by Apelt (1961), and for $R = 2, 4, 10$, and 15 by Keller & Takami (1966, pp. 115–140). There are also the solutions of Allen & Southwell (1955) by relaxation methods for $R = 0$ (sic), 1, 10, 100, and 1000. Their results, however, are suspect, as pointed out by Kawaguti (1959). Finally, Kawaguti & Jain (1965) obtained steady-state solutions for $R = 1$, 10, 20, 30, 40, and 50 as the limit of solutions of the unsteady Navier–Stokes equations.

The present semi-analytic solution to the full Navier–Stokes equations makes it possible to describe accurately the flow field about a circular cylinder over a wide range of Reynolds numbers without resorting either to full numerical solution or to experiment. While results are given for Reynolds numbers from order 10^{-1} to order 10, the method can be applied to both higher and lower Reynolds numbers without modification. Analysis proceeds employing the method of series truncation to reduce the governing partial differential equations of motion to a system of ordinary differential equations which can be integrated numerically, a simpler task than solving the original governing equations numerically.

One other semi-analytic solution for the low Reynolds number flow past a circular cylinder is documented, namely that of Dennis & Shimshoni (1965). Their solution uses a somewhat different approach from the present solution, and the validity of their results is questionable.

2. Analysis

The problem under consideration here is that of the incompressible flow past a circular cylinder at moderate Reynolds number. The flow is assumed to be steady and two-dimensional, with uniform free-stream velocity U_∞. The viscosity μ is also assumed constant. The constant fluid density is denoted by ρ. For a circular geometry the natural co-ordinates are cylindrical; the polar co-ordinate system employed, with the angle θ measured from the upstream axis, is depicted in figure 1. The fundamental length for the problem is the radius of the cylinder a, to which all lengths are referred.

The physical flow variables are non-dimensionalized by reference to free-stream conditions. Hence, u and v are the velocity components along r and θ referred to U_∞, and p is the pressure referred to $\rho U_\infty{}^2$.

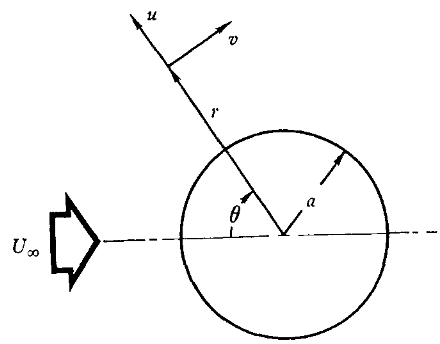

FIGURE 1. Polar co-ordinate system.

Flow equations and boundary conditions

Under the assumptions of steady, laminar, incompressible flow the governing differential equations expressing conservation of mass and momentum in the polar co-ordinates of figure 1 are

$$\frac{\partial}{\partial r}(ru)+\frac{\partial v}{\partial \theta} = 0, \tag{1}$$

$$u\frac{\partial u}{\partial r}+\frac{v}{r}\frac{\partial u}{\partial \theta}-\frac{v^2}{r}+\frac{\partial p}{\partial r} = \frac{2}{R}\left(\frac{\partial^2 u}{\partial r^2}+\frac{1}{r}\frac{\partial u}{\partial r}+\frac{1}{r^2}\frac{\partial^2 u}{\partial \theta^2}-\frac{u}{r^2}-\frac{2}{r^2}\frac{\partial v}{\partial \theta}\right), \tag{2}$$

and

$$u\frac{\partial v}{\partial r}+\frac{v}{r}\frac{\partial v}{\partial \theta}+\frac{uv}{r}+\frac{1}{r}\frac{\partial p}{\partial \theta} = \frac{2}{R}\left(\frac{\partial^2 v}{\partial r^2}+\frac{1}{r}\frac{\partial v}{\partial r}+\frac{1}{r^2}\frac{\partial^2 v}{\partial \theta^2}+\frac{2}{r^2}\frac{\partial u}{\partial \theta}-\frac{v}{r^2}\right), \tag{3}$$

where R is the Reynolds number defined with the diameter $2a$ of the circular cylinder as the characteristic length, i.e.

$$R = (2\rho U_\infty a)/\mu. \tag{4}$$

It is possible to reduce the system of equations (1), (2) and (3) to a single equation by introducing the stream function ψ, defined such that

$$u = -\frac{1}{r}\frac{\partial \psi}{\partial \theta}, \tag{5}$$

$$v = \partial\psi/\partial r. \tag{6}$$

Then the governing equation of motion becomes

$$\nabla^4\psi+\frac{R}{2r}\left(\frac{\partial \psi}{\partial \theta}\frac{\partial}{\partial r}-\frac{\partial \psi}{\partial r}\frac{\partial}{\partial \theta}\right)\nabla^2\psi = 0, \tag{7}$$

where

$$\nabla^2 = \frac{\partial^2}{\partial r^2}+\frac{1}{r}\frac{\partial}{\partial r}+\frac{1}{r^2}\frac{\partial^2}{\partial \theta^2}. \tag{8}$$

The boundary conditions result from the conditions of zero velocity at the body surface:

$$\text{at} \quad r = 1, \quad \psi(r,\theta) = 0, \tag{9}$$

$$(\partial\psi/\partial r)(r,\theta) = 0 \tag{10}$$

and from the condition of uniform flow far upstream from the body:

$$\text{as} \quad r \to \infty, \quad \psi(r,\theta) \sim r\sin\theta. \tag{11}$$

The single partial differential equation in ψ, (7), in conjunction with the boundary conditions, (9), (10) and (11), constitutes an exact, well-posed, mathematical description of the flow problem under consideration.

Method of solution

The problem is solved by application of the semi-analytic method of series truncation. This method has been used extensively in treatment of the hypersonic blunt-body problem by M. D. Van Dyke and his students at Stanford University (see Van Dyke 1965). Also, Van Dyke (1964*a*, 1965) briefly considered the incompressible, viscous flow past a circular cylinder. A recent application is Davis's (1967) investigation of the laminar incompressible flow past a semi-infinite flat plate.

The method of series truncation is a successive approximation procedure which treats an elliptic partial differential equation as if it were parabolic or hyperbolic. The dependent variable is expanded in one co-ordinate, which plays the role of a time-like variable, and backward influence in the resultant system of ordinary differential equations is eliminated by series curtailment.

A classic example of the utility of such a co-ordinate expansion for a parabolic problem is the Blasius series for the laminar boundary layer on a smooth, plane or axisymmetric body (Schlichting 1960, p. 146), where the stream function is formally expanded in powers of the longitudinal boundary-layer co-ordinate, with undetermined functions of the normal co-ordinate alone as coefficients. Substituting the Blasius series into the boundary-layer equation and equating like-order terms yields a coupled sequence of ordinary differential equations which can be successively integrated numerically. Such a procedure is successful, physically, because the boundary layer at a point is unaffected by the downstream flow so that there is no backward influence, and, mathematically, because the boundary-layer equations are parabolic.

A basically analogous procedure is employed for the solution of an elliptic problem by the method of series truncation, with one notable discrepancy introduced by the effects of the ellipticity. Unlike parabolic and hyperbolic equations, elliptic equations characteristically display upstream or backward influence; hence, successive integration of the system of ordinary differential equations resulting from a co-ordinate expansion is not possible. Nonetheless, by making suitable approximating assumptions upon those terms indicating backward influence in the ordinary differential equations, an elliptic problem can be treated as a pseudo-hyperbolic or pseudo-parabolic problem. This is the crux of the method of series truncation.

Application to the present problem

The stream function is formally expanded in a Fourier sine series

$$\psi(r,\theta) = f_1(r)\sin\theta + f_2(r)\sin 2\theta + \ldots, \tag{12}$$

with the functions $f_1(r), f_2(r), \ldots$ as yet unknown. Symmetry and antisymmetry of the velocity components u and v, respectively, indicate that the Fourier series is composed of sine terms alone.

The usefulness of the form of the expansion for ψ is affirmed by several considerations. That such a representation is efficacious near the surface of the body at low Reynolds number is clear from the Stokes approximation (see Van Dyke 1964*b*, p. 149), where the solution is an unknown multiple of the first term, and formal iteration adds a likewise unknown multiple of the second term. Furthermore, the first term is in accord with the boundary condition far upstream from the body.

Expansion (12) is subsequently substituted into the governing partial differential equation. Then collecting like Fourier coefficients yields a system of the following form:

$$[T_1(r, f_1, f_2, f_3, \ldots; R)]\sin\theta + [T_2(r, f_1, f_2, f_3, \ldots; R)]\sin 2\theta + T_3\sin 3\theta + T_4\sin 4\theta + \ldots = 0, \tag{13}$$

where the T_j $(j = 1, 2, \ldots)$ are non-linear ordinary differential expressions. Satisfaction of (13) for arbitrary θ requires $T_j \equiv 0$ for $j = 1, 2, \ldots$.

The subscript j is said to represent the jth-order problem. Hence, the first-order problem is governed by the ordinary differential equation $T_1 = 0$, the second-order problem by $T_2 = 0$, etc. The effects of ellipticity are readily visible here, since the problem of each order contains functions belonging to higher-order problems; on the other hand, as previously seen, parabolic and hyperbolic problems yield an independent first-order problem, and higher-order problems which can be solved entirely in terms of the problems of preceding orders.

At this point, an apparent impasse has been reached. The problem of each order is indeterminate, possessing infinitely more unknowns than equations. It is possible, however, to circumvent the difficulty by arbitrarily setting the undesirable functions equal to zero. Indeed, it is from this operation that the method of series truncation derives its name, since such a procedure is equivalent to successive truncation of series (12). In this manner, the problem becomes solvable, but only by the introduction of an approximation. The assumption that higher-order excess unknowns are zero is somewhat brutal, and it would be more refined to relate them in some manner to the lower-order terms. Kao (1964) pursued this reasoning with excellent results. Nonetheless, previous applications of the method have indicated that summary truncation produces good results as long as the form of the expansions for the dependent variables is chosen judiciously.

For the actual solution by the method of series truncation the first truncation involves solving $T_1 = 0$ with $f_2 = f_3 = \ldots \equiv 0$ and appropriate boundary conditions, thereby yielding an approximate solution to the first-order problem. For the second truncation, the two equations $T_1 = 0$ and $T_2 = 0$ are solved simultaneously with $f_3 = f_4 = \ldots \equiv 0$ and applicable boundary conditions. This gives approximate solutions to both the first- and second-order problems, now with non-zero f_2. Ensuing truncations are calculated in the same manner until satisfactory convergence between succeeding approximate solutions to the various-order problems is obtained.

For the present problem five truncations have been calculated. The first truncation leads identically to the Stokes approximation and the associated non-uniformity at infinity that prevents imposing the upstream boundary condition (see Van Dyke 1964*b*). This defect disappears in the higher truncations.

The second truncation system of equations ($T_1 = 0$ and $T_2 = 0$ with $f_3 = f_4 = \ldots \equiv 0$ and applicable boundary conditions) is:

$$f_1^{\mathrm{iv}} + \frac{2}{r}f_1''' - \frac{3}{r^2}f_1'' + \frac{3}{r^3}f_1' - \frac{3}{r^4}f_1 + \frac{R}{2r}\left[\tfrac{1}{2}f_1\left(f_2''' + \frac{1}{r}f_2'' - \frac{5}{r^2}f_2' + \frac{8}{r^3}f_2\right)\right.$$
$$-\frac{1}{2}f_2'\left(f_1'' + \frac{1}{r}f_1' - \frac{1}{r^2}f_1\right) - f_2\left(f_1''' + \frac{1}{r}f_1'' - \frac{2}{r^2}f_1' + \frac{2}{r^3}f_1\right)$$
$$\left. + f_1'\left(f_2'' + \frac{1}{r}f_2' - \frac{4}{r^2}f_2\right)\right] = 0, \tag{14}$$

$$f_2^{\mathrm{iv}} + \frac{2}{r}f_2''' - \frac{9}{r^2}f_2'' + \frac{9}{r^3}f_2' + \frac{R}{2r}\left[\frac{1}{2}f_1\left(f_1''' + \frac{1}{r}f_1'' - \frac{2}{r^2}f_1' + \frac{2}{r^3}f_1\right)\right.$$
$$\left. - \frac{1}{2}f_1'\left(f_1'' + \frac{1}{r}f_1' - \frac{1}{r^2}f_1\right)\right] = 0, \tag{15}$$

$$f_1(1) = f_1'(1) = f_2(1) = f_2'(1) = 0, \tag{16)–(19}$$

$$f_1(r) \sim r \quad \text{as} \quad r \to \infty, \tag{20}$$

$$f_2(r) = o(r) \quad \text{as} \quad r \to \infty, \tag{21}$$

where primes denote differentiation with respect to r. This system was solved by numerical integration. The method of numerical solution is described below.

The third, fourth and fifth truncations were calculated by obvious extension of the previously described procedure. The corresponding systems of ordinary differential equations are given by Underwood (1968).

Technique for numerical solution

After a number of numerical schemes for the solution of non-linear two-point boundary-value problems (e.g. quasi-linearization) had been surveyed, it was decided that programming complexity, computer core storage, and machine run time could be optimized with a hybrid contrivance reflecting the basic character of the equations involved in the current truncation problems. The method finally selected was an iterative linearization procedure which can be illustrated by closer examination of the second truncation equations (14) and (15). These equations may be rewritten in the form:

$$f_1^{\mathrm{iv}} + \frac{2}{r}f_1''' - \frac{3}{r^2}f_1'' + \frac{3}{r^3}f_1' - \frac{3}{r^4}f_1 = F_1(r, f_1, f_2; R), \tag{22}$$

$$f_2^{\mathrm{iv}} + \frac{2}{r}f_2''' - \frac{9}{r^2}f_2'' + \frac{9}{r^3}f_2' = F_2(r, f_1; R). \tag{23}$$

The left-hand sides of (22) and (23) are fourth-order, linear, ordinary differential expressions. If a prior estimate of the form of $f_1(r)$ and $f_2(r)$ is used in evaluating $F_1(r, f_1, f_2; R)$ and $F_2(r, f_1; R)$, there results a system of uncoupled, linear ordinary differential equations to solve. For each linear problem it is possible to find a particular solution and add to it a homogeneous solution (easily found analytically) to meet the boundary conditions. The solutions to the linear problems are used to re-estimate $F_1(r; R)$ and $F_2(r; R)$, and another solution to the linear system follows. Upon agreement between estimates of the right-hand sides of the equations and the ensuing solutions to the linearized problems, the desired profiles for $f_1(r)$ and $f_2(r)$ have been found.

Particular solutions to the linearized equations were found using a fourth-order Runge–Kutta integration programme. In obtaining converged profiles, the iteration procedure was found to be very sensitive to the initial profile approximations. Therefore, the estimated distribution $\bar{f}_n(r)$ and the calculated value $f_n(r)$ were weighted to obtain a new estimated value $\bar{f}_n(r)_{\text{new}}$ for the next iteration as follows:

$$\bar{f}_n(r)_{\text{new}} = \bar{f}_n(r) + \omega(f_n(r) - \bar{f}_n(r)). \tag{24}$$

The weighting factor ω was varied according to the relation

$$\omega = KP, \tag{25}$$

with the value of K increased by one after L iterations. L depended upon the truncation and the Reynolds number; the appropriate value was obtained from experience. The value of P also depended upon the truncation and the Reynolds number, with values between 0·1 and 0·01 being typical. The various $f_n(r)$ profiles were considered to have been determined when the relative differences in the calculated values of $f_n'''(1)$ between the ith and $(i+1)$th iterations were less than 10^{-5}, i.e. when

$$\frac{|f_n'''(1)_{i+1} - f_n'''(1)_i|}{|f_n'''(1)_i|} < 10^{-5}. \tag{26}$$

Another consideration arising in the numerical solution of the second and higher truncations is that of optimum imposition of the asymptotic infinity boundary conditions. The conditions as given by (20) and (21) can be replaced by others that have the two advantages of being attained with exponentially, rather than algebraically, decaying error, and of permitting integration through a reasonably small interval. These are based upon the asymptotic forms of the solutions. The asymptotic behaviour far from the body for the governing sets of ordinary differential equations can be found by constructing the perturbation solutions about the free stream. As would be expected, such an analysis indicates that the asymptotic forms of the desired solutions are the same as for the Oseen model. Fortunately, the Oseen model for this problem has been investigated by Van Dyke (1964*a*). He argued, and it was well confirmed by his numerical integrations, that for the Oseen model the following asymptotic forms are valid far from the body to within exponentially small terms:

$$f_1(r) \sim r + \frac{a}{r}, \quad f_2(r) \sim b + \frac{c}{r^2}, \tag*{(27), (28)}$$

where a, b, and c are unknown constants. With these asymptotic forms assumed valid for the present problem, it is then possible to form the alternative linearly independent relations:

$$\frac{f_1(r)}{r}+f_1'(r) \sim 2, \quad 2f_1'(r)+rf_1''(r) \sim 2, \tag{29), (30}$$

$$3f_2'(r)+rf_2''(r) \sim 0, \quad 4f_2''(r)+rf_2'''(r) \sim 0. \tag{31), (32}$$

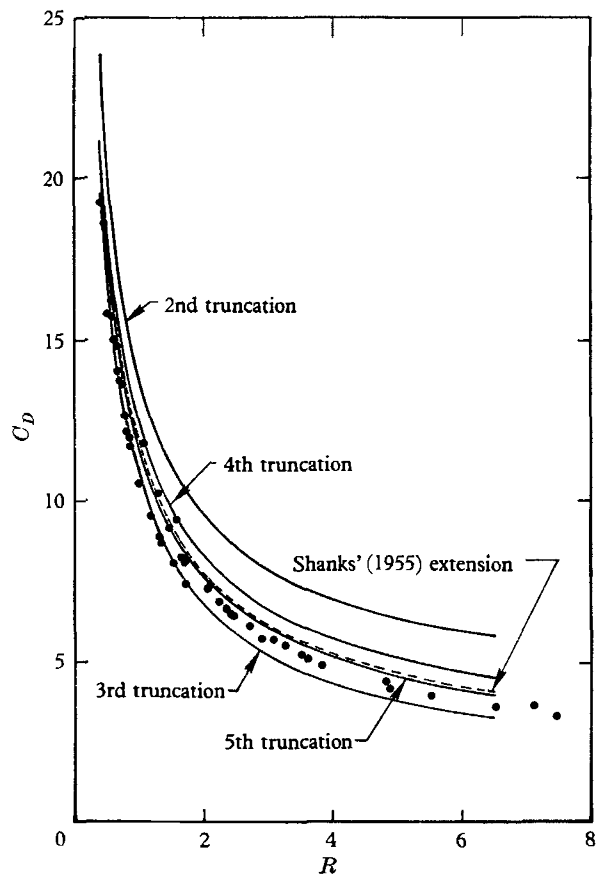

FIGURE 2. Drag coefficient *vs.* Reynolds number for second, third, fourth and fifth truncations. ●, Tritton's (1959) data.

In the actual numerical solution, (29)–(32) were used as the infinity boundary conditions and were imposed at some sufficiently large radius, r_∞. Experimentation indicated that these conditions determined the required profiles to four significant figures when the numerical integration was carried to $Rr_\infty \approx 40$.

The requisite numerical computations for the current investigation were programmed in FORTRAN IV (H level) and were performed on the IBM System 360/67 automatic digital computer of the Stanford Computation Center. The calculated wall values for the $f_n(r)$ profiles in the second, third, fourth, and fifth truncations are given by Underwood (1968).

Onset of separated flow; drag and pressure coefficients

Experimental studies have indicated the existence of a critical value of the Reynolds number above which separated flow results, with its accompanying standing eddies at the rear of the cylinder. Since these vortices are perhaps the most readily observable flow-field characteristic when they exist, it is of great interest to verify their occurrence with the present theory and to determine accurately the value of the separation Reynolds number. A Taylor series expansion of the stream function near the surface of the body indicates that for the nth truncation the onset of separation occurs at the Reynolds number for which

$$\sum_{i=1}^{n} i(-1)^{i+1} f_2''(1) = 0. \tag{33}$$

The left-hand side of (33) will be referred to as the 'separation parameter' for notational convenience.

In past studies of the low Reynolds number flow past a circular cylinder the drag coefficient has been the most closely examined flow parameter. The current semi-analytic approach, unlike full numerical solution, gives a simple expression for the calculation of drag. Manipulation of the governing equations shows that only the first term in the Fourier expansion of $\psi(r,\theta)$ contributes to the drag, and the drag coefficient C_D is given by

$$C_D = \frac{\text{drag}}{\rho U_\infty^2} = -\frac{2\pi}{R} f_1'''(1). \tag{34}$$

Similarly, combination of the governing equations reveals that the pressure coefficient C_p for the nth truncation is

$$\begin{aligned} C_p \equiv \frac{p_\theta - p_\infty}{\frac{1}{2}\rho U_\infty^2} &= \frac{4}{R} \sum_{j=1}^{n} \left\{ \frac{1}{j} [f_j'''(1) + f_j''(1)] (1 - \cos j\theta) \right\} \\ &+ \frac{4}{R} \int_{r=1}^{\infty} \left\{ \sum_{j=1}^{n} \left[\frac{j}{r} f_j''(r) + \frac{j}{r^2} f_j'(r) - \frac{j^3}{r^3} f_j(r) \right] \right\} dr \\ &+ 2 \int_{r=1}^{\infty} \left[\sum_{j=1}^{n} \frac{j}{r} f_j(r) \right] \left\{ \sum_{j=1}^{n} \left[\frac{j}{r} f_j'(r) - \frac{j}{r^2} f_j(r) \right] \right\} dr, \end{aligned} \tag{35}$$

where p_θ is the dimensional surface pressure at an angle θ along the body, and p_∞ is the free-stream pressure. The required integrations in (35) were performed numerically using values from the calculated profiles for the various truncations.

3. Discussion of results

Results of present study

Figures 2 and 3 show the drag coefficient and separation parameter, respectively, plotted against Reynolds numbers ranging from 0·4 to 6·5 for the second, third, fourth and fifth truncations. The truncations constitute an alternating sequence, which appears to converge quite rapidly. The actual drag coefficient and separation Reynolds number yielded by the present theory evidently lie between the values predicted by the fourth and fifth truncations.

It is clear that convergence of the sequence has not been obtained by the calculation of the first five truncations. Nonetheless, the information contained in these truncations makes it possible to extract accurate values by application of the non-linear Shanks' transformation (Shanks 1955). If S_{n-1}, S_n, and S_{n+1} are three successive approximations to a quantity, a revised value is given by

$$S \approx \frac{S_{n+1}S_{n-1} - S_n^2}{S_{n+1} + S_{n-1} - 2S_n}. \tag{36}$$

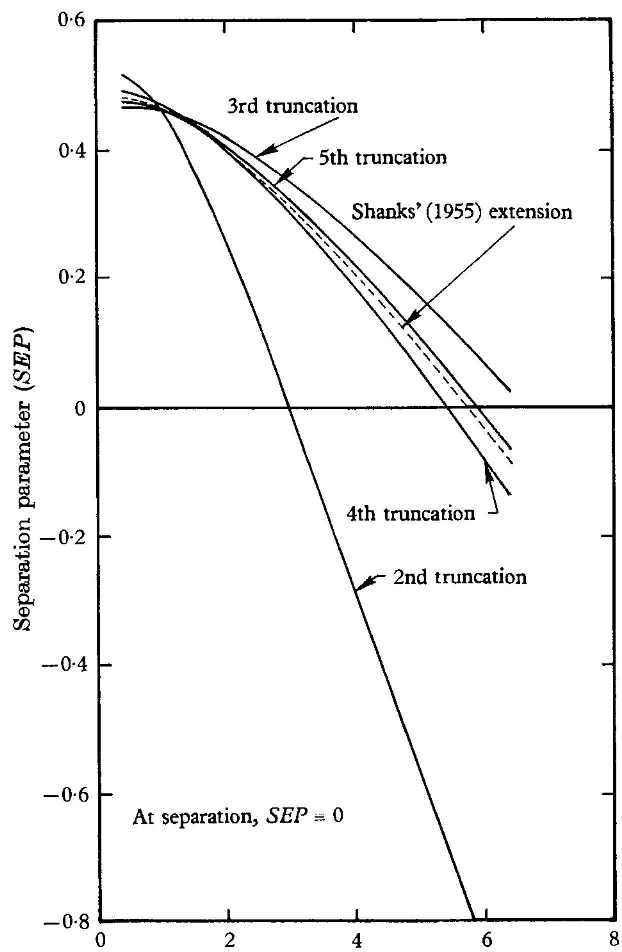

FIGURE 3. Separation parameter *vs.* Reynolds number for second, third, fourth and fifth truncations.

Applying this transformation to the second, third, and fourth truncations and to the third, fourth, and fifth truncations gives values of the drag coefficient and the separation parameter which agree to three significant figures. These are plotted as the Shanks' extension in figures 2 and 3. Examination of the figures suggests that fifth truncation values give a good approximation to the converged solutions represented by the Shanks' extension.

Since algebraic complexity, and consequently computer run-time increase considerably with each successive truncation, it is desirable to effect the most rapid convergence possible. The form of the expansion (12) for the dependent variable $\psi(r, \theta)$ is important in determining convergence. Although the present

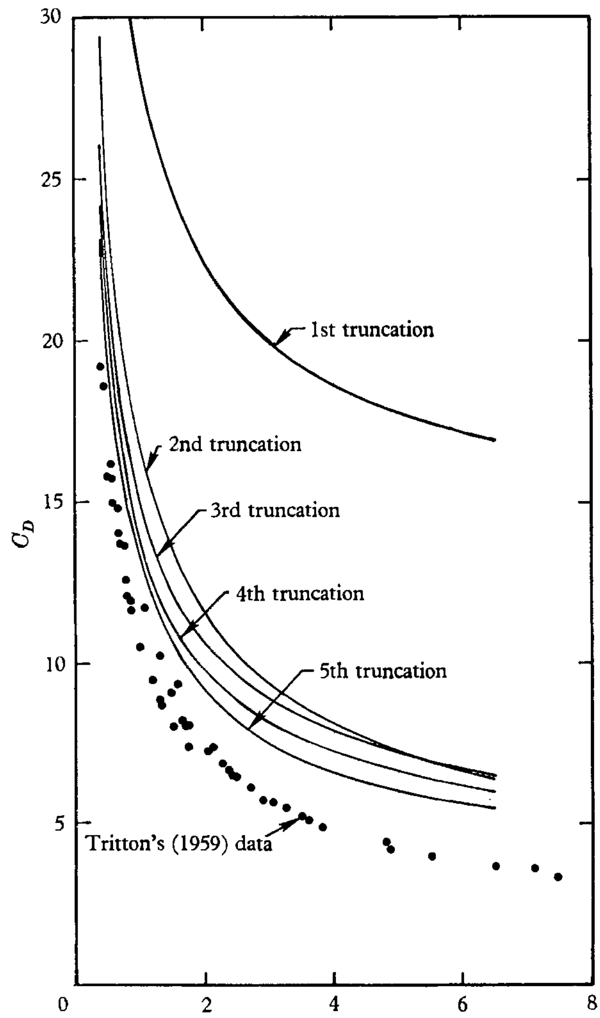

FIGURE 4. Drag coefficient *vs.* Reynolds number for first five truncations in powers of sin θ.

expansion gives satisfactory convergence, improvements are undoubtedly possible. It is clear that the more closely $f_1(r)$ represents the actual solution, the more convergence is improved. In addition, obtaining a first truncation that does not lead to Stokes' paradox seems desirable. To this end, Van Dyke (1964*a*) suggested substituting (12) for $\psi(r, \theta)$ into the Navier–Stokes equations, and then expanding the result in powers of $\sin\theta$. Equating like powers of $\sin\theta$ led to a truncation problem. Investigation of this idea shows, however, that the resulting convergence is decidedly inferior to the convergence in the current variables. Figures 4 and 5 show the drag coefficient and separation parameter, respectively, for the first five truncations in powers of $\sin\theta$. The separation parameter, in particular, converges extremely slowly in these variables. As the expansion in powers of $\sin\theta$ is an expansion which is strictly valid only in the vicinity of the cylinder's upstream stagnation point and separation occurs to the rear of the cylinder, this behaviour might be expected.

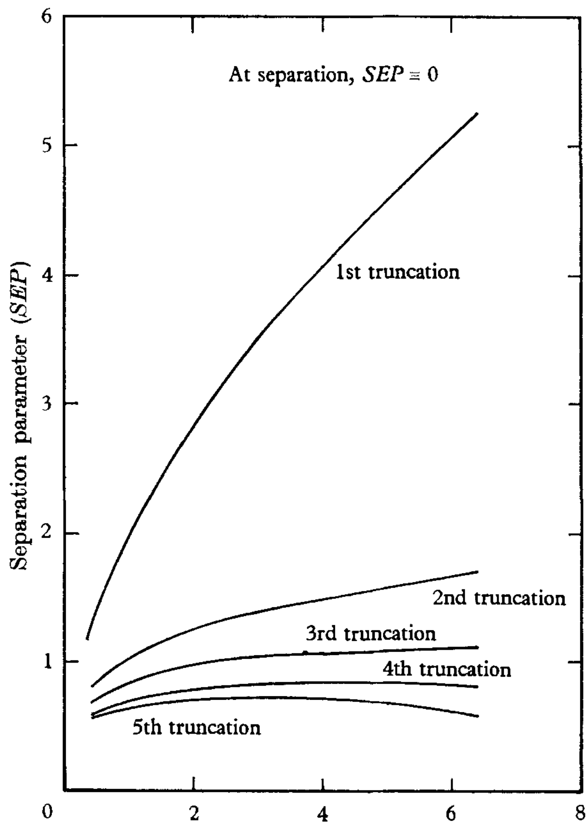

FIGURE 5. Separation parameter *vs.* Reynolds number for first five truncations in powers of $\sin\theta$.

Since the fifth truncation has been seen to approximate the converged solution adequately for the present problem, properties of the flow field about a circular cylinder can be found by further examination of fifth truncation results. Figure 6 gives the pressure coefficient for representative Reynolds numbers between 0·4 and 10·0. It is well known that for $R \ll 1$ the minimum pressure occurs at the rear stagnation point, but as R increases the point of minimum pressure moves upstream. This behaviour is noted in the present solution.

Figures 7–10 show streamlines for the flow past a circular cylinder at Reynolds numbers of 0·4, 1·6, 6·4 and 10·0, respectively. At very low Reynolds numbers the flow past a circular cylinder displays fore-and-aft symmetry near the body, but distinct asymmetry farther out. As R increases, however, the asymmetry becomes more pronounced and affects the flow near the body. Above the separation Reynolds number, standing eddies form behind the cylinder, becoming more pronounced as R grows.

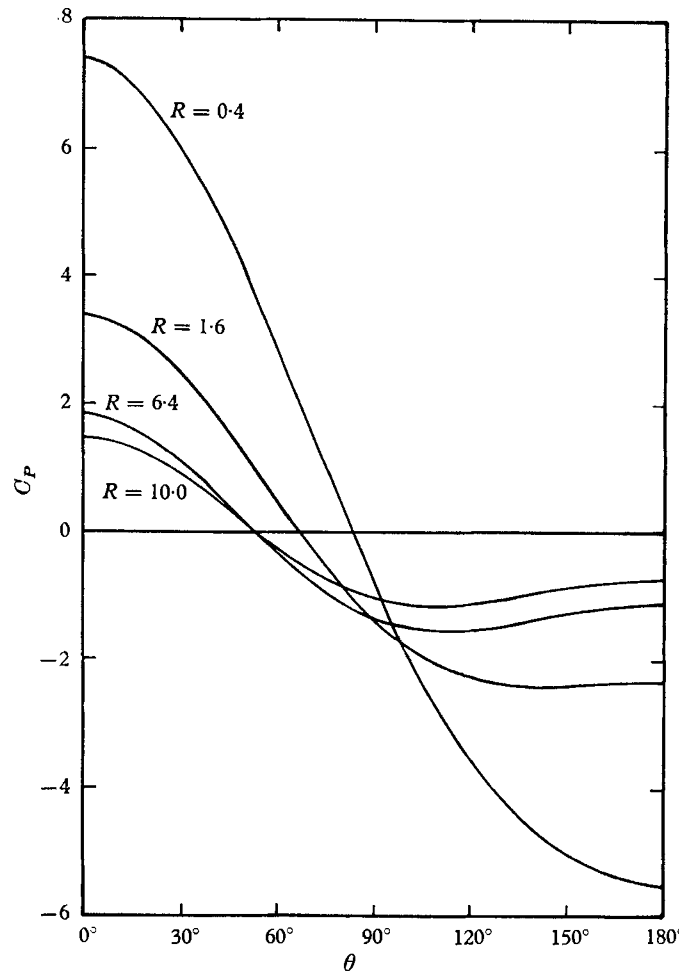

FIGURE 6. Pressure coefficient calculated from fifth truncation solutions for $0{\cdot}4 \leqslant R \leqslant 10{\cdot}0$.

Comparison of results

Where possible, results of the present study have been compared with results of previous investigations. Figure 11 presents a comparison of the variation of the drag coefficient predicted by the present theory with that from existing theoretical and numerical solutions and experimental data. The inadequacy of the matched asymptotic expansion solutions of Kaplun (1957) and Proudman & Pearson (1957) above $R = 2$ is evident, although the former's formulation of the drag coefficient is obviously preferable. Lamb's (1911) approximate solution of the Oseen equations is adequate at low Reynolds numbers, but it too fails above

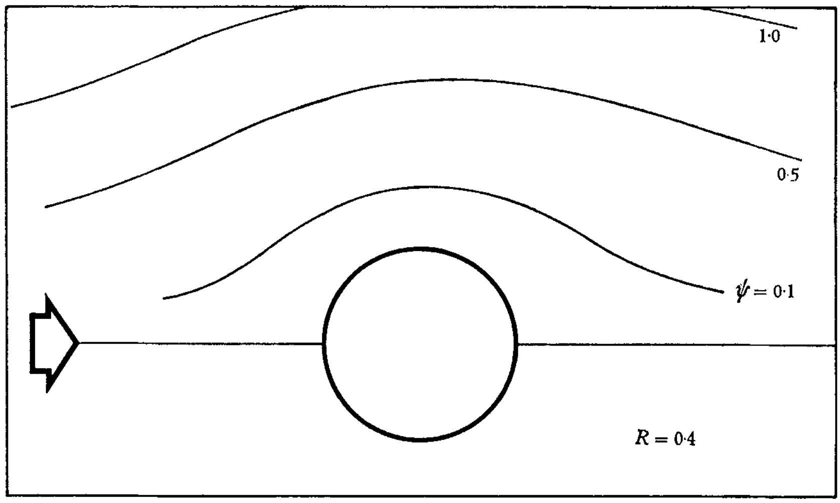

FIGURE 7. Streamlines calculated from fifth truncation for $R = 0\cdot4$.

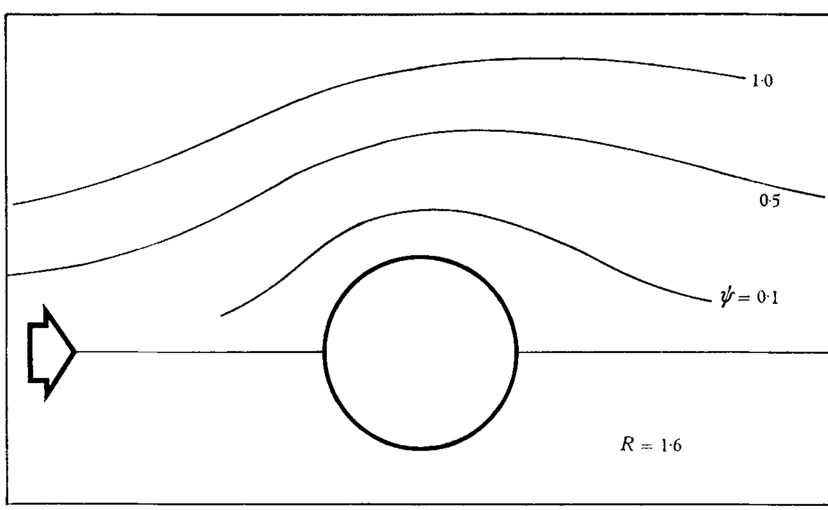

FIGURE 8. Streamlines calculated from fifth truncation for $R = 1\cdot6$.

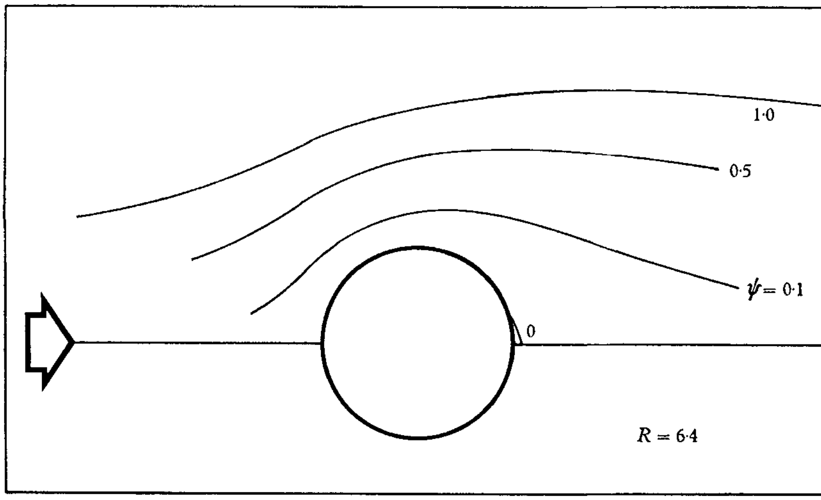

FIGURE 9. Streamlines calculated from fifth truncation for $R = 6{\cdot}4$.

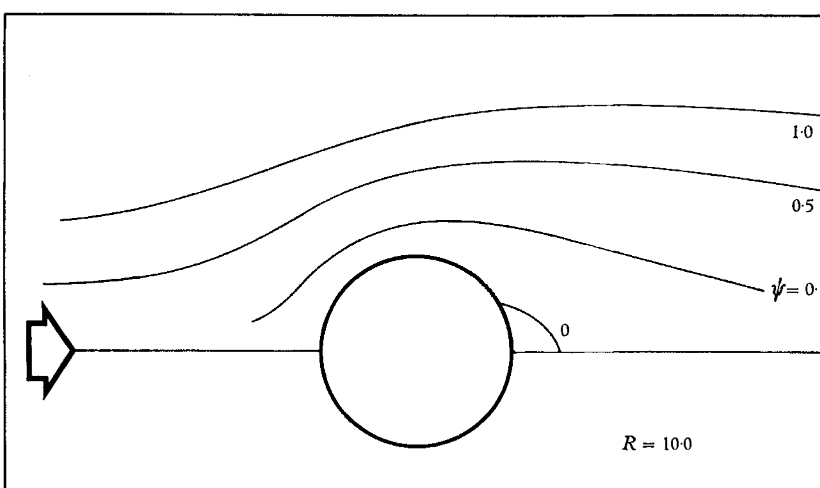

FIGURE 10. Streamlines calculated from fifth truncation for $R = 10{\cdot}0$.

$R = 2$. The full Oseen solution approaches Tritton's (1959) experimental data for low Reynolds numbers; however, the agreement worsens as R increases. The present solution by the method of series truncation compares favourably with Tritton's data over the entire range of Reynolds numbers. The drag coefficient approaches the correct limit for $R \ll 1$ and does not diverge from the experimental data for $R > 1$.

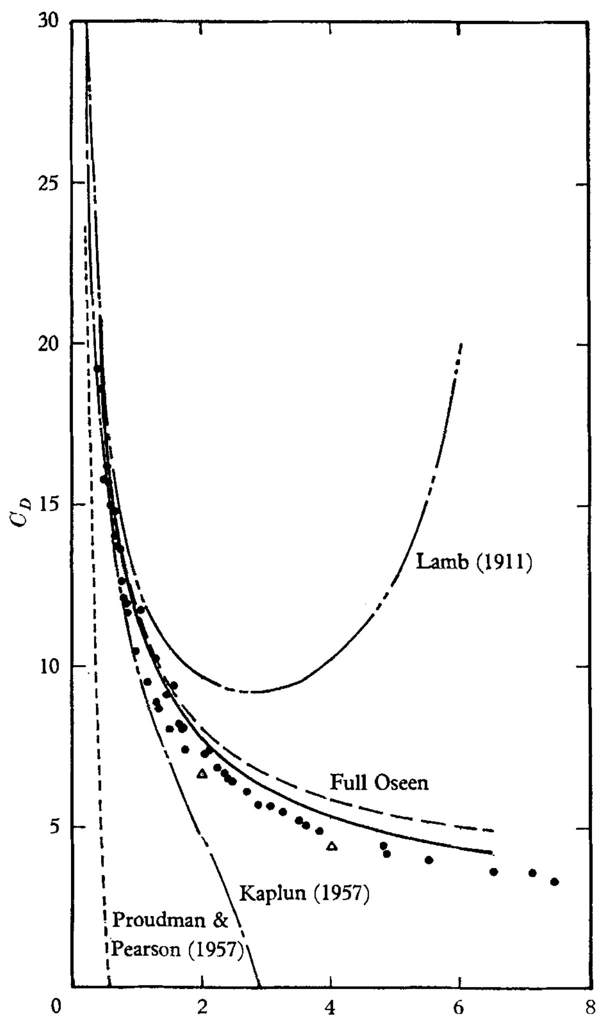

FIGURE 11. Comparison of drag coefficient *vs*. Reynolds number from present theory with existing theoretical and numerical solutions and experimental data. ●, Tritton's (1959) data; ——, Shanks' (1955) extension of present solution; △, Keller & Takami (1966) (numerical).

Accurate determination of the Reynolds number at which separation first occurs at the rear of the cylinder was one of the primary aims of the present study. As seen from figure 3, the present analysis indicates that the separation Reynolds number lies within the range $5{\cdot}45 < R < 5{\cdot}86$. Using the Shanks' extension gives

$R = 5{\cdot}75$ as a more refined estimate. This is consistent with the value $R = 5$ found experimentally by Taneda (1956).

The length of the standing eddy from the fifth truncation is compared in figure 12 with previous experimental and numerical values. The eddy length is seen to vary in an approximately linear manner with R, and the slope corresponds to that of Taneda's (1956) experimental data. The fact that the fifth truncation

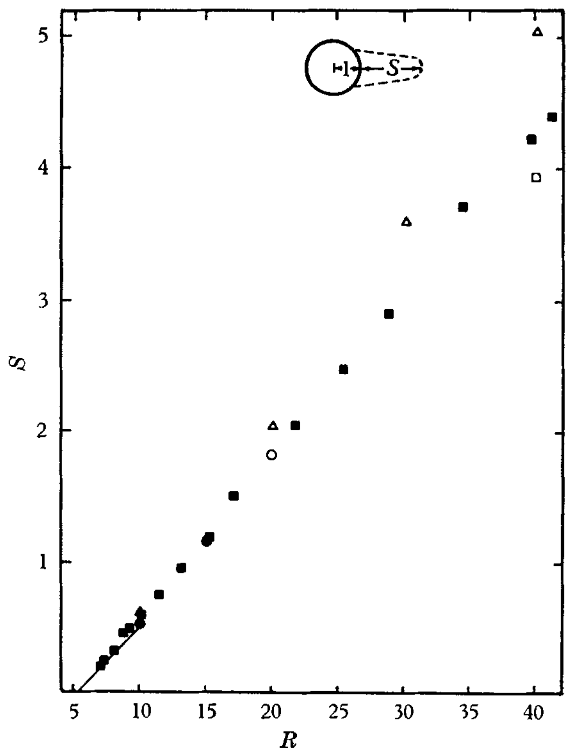

FIGURE 12. Comparison of fifth truncation eddy length with other existing data. ■, Taneda (1956); ●, Keller & Takami (1966); ○, Thom (1933); □, Kawaguti (1953); △, Kawaguti & Jain (1965); ——, present solution.

values lie slightly below the experimental points should be expected, since it is apparent from figure 3 that the fifth truncation underestimates the extent of separated flow.

As a further comparison, figure 13 shows the pressure distribution for $R = 10{\cdot}0$ calculated from the fifth truncation, from Keller & Takami's (1966) full numerical solution, and from Kawaguti & Jain's (1965) time-dependent numerical solution. Agreement is good, especially along the upstream portions of the circular cylinder.

4. Conclusions

The viscous, incompressible flow at low Reynolds number past a circular cylinder provides a severe test of the method of series truncation. Not only is the governing equation highly elliptic, but the flow disturbances extend far from the body. Nevertheless, if the form of the expansion for the dependent variable

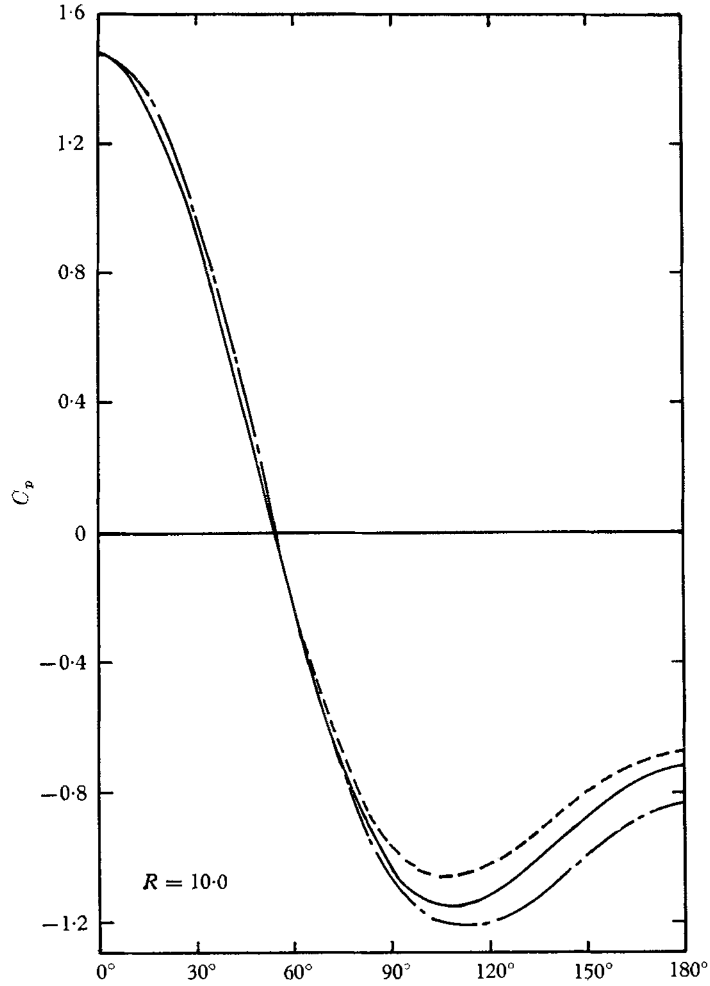

FIGURE 13. Pressure coefficient for $R = 10{\cdot}0$. ——, fifth truncation; – – –, Keller & Takami's (1966) numerical solution; — – —, Kawaguti & Jain's (1965) numerical solution.

is chosen carefully, satisfactory convergence is obtained with the method; and the flow characteristics can be determined accurately.

Development of the present solution has suggested several general rules to observe in selecting a form for the expansion of the dependent variable. First, attempts should be made to select an expansion which is valid throughout the flow field. If, however, it becomes necessary to expand the series for the dependent variable asymptotically to obtain a truncation problem, that asymptotic expansion should be postponed as long as possible in the analysis.

Thus, for the present problem a Fourier expansion (12) for the stream function was chosen, since such an expansion is valid throughout the flow domain. In an attempt to rectify the primary deficiency of the resulting truncations (namely, an insoluble first truncation) Van Dyke (1964*a*) proposed a further expansion in powers of $\sin\theta$. The Fourier series could be expanded in powers of $\sin\theta$ and then substituted into the Navier–Stokes equations, or the order of operations could be reversed. The operations are not commutative, and the latter sequence is preferable, since it preserves generality as long as possible and avoids asymptotic expansion until a later stage of the analysis. Convergence of successive truncations, though, is markedly superior with the stream function expanded in a Fourier series alone, without further asymptotic expansions. In this manner, the greatest generality possible is maintained.

Whereas numerical solutions of the Navier–Stokes equations require integration of partial differential equations, the present semi-analytic computation possesses the distinct advantage of resulting in the numerical integration of a system of ordinary differential equations. The mathematical theory for treatment of ordinary differential equations is much more advanced than that for partial differential equations. For example, estimates of the error introduced by numerical integration are readily available for techniques dealing with ordinary differential equations, and the integration mesh is easily altered to keep error within arbitrary bounds. Again, questions of stability tend to be critical in numerical solution of partial differential equations.

In the present investigation the method of series truncation is used to analyze the flow field about a circular cylinder for Reynolds numbers from order 10^{-1} to order 10, although the applicability of the method is by no means limited to this régime. Fifth truncation solutions are seen to give a very good approximation to the actual flow field, while a typical fifth truncation calculation necessitates on the order of 25 % of the computer time required for the corresponding full numerical solution. Furthermore, present results bear semi-analytic representation.

The present work was supported by the U.S. Air Force Office of Scientific Research under Contract No. AF 49(638)-1274. The author is indebted to M. D. Van Dyke for invaluable counsel and criticisms.

REFERENCES

Allen, D. N. de G. & Southwell, R. V. 1955 Relaxation methods applied to determine the motion, in two dimensions, of a viscous fluid past a fixed cylinder. *Quart. J. Mech. Appl. Math.* **8**, 129–145.

Apelt, C. J. 1961 The steady flow of a viscous fluid past a circular cylinder at Reynolds numbers 40 and 44. *Aero. Res. Counc. Lond. R & M* no. 3175.

Davis, R. T. 1967 Laminar incompressible flow past a semi-infinite flat plate. *J. Fluid Mech.* **27**, 691–704.

Dennis, S. C. R. & Shimshoni, M. 1965 The steady flow of a viscous fluid past a circular cylinder. *Aero. Res. Counc. Lond. Current Paper* no. 797.

KAO, H. C. 1964 Hypersonic viscous flow near the stagnation streamline of a blunt body. *AIAA J.* **2**, 1892–1897.

KAPLUN, S. 1957 Low Reynolds number flow past a circular cylinder. *J. Math. Mech.* **6**, 595–603.

KAWAGUTI, M. 1953 Numerical solution of the Navier–Stokes equations for the flow around a circular cylinder at Reynolds number 40. *J. Phys. Soc. Japan*, **8**, 747–757.

KAWAGUTI, M. 1959 Note on Allen & Southwell's paper 'Relaxation methods applied to determine the motion, in two dimensions, of a viscous fluid past a fixed cylinder'. *Quart. J. Mech. Appl. Math.* **12**, 261–263.

KAWAGUTI, M. & JAIN, P. 1965 Numerical study of a viscous fluid past a circular cylinder. University of Wisconsin, MRC Summary Report no. 590.

KELLER, H. B. & TAKAMI, H. 1966 Numerical studies of steady viscous flow about cylinders. *Numerical Solutions of Nonlinear Differential Equations* (ed. D. Greenspan). New York: Wiley.

LAMB, H. 1911 On the uniform motion of a sphere through a viscous fluid. *Phil. Mag.* **21**, 112–121.

PROUDMAN, I. & PEARSON, J. R. A. 1957 Expansions at small Reynolds numbers for the flow past a sphere and a circular cylinder. *J. Fluid Mech.* **2**, 237–262.

SCHLICHTING, H. 1960 *Boundary Layer Theory* (4th ed.). New York: McGraw-Hill.

SHANKS, D. 1955 Nonlinear transformations of divergent and slowly convergent sequences. *J. Math Phys.* **34**, 1–42.

TANEDA, S. 1956 Experimental investigation of the wakes behind cylinders and plates at low Reynolds numbers. *J. Phys. Soc. Japan*, **11**, 302–307.

THOM, A. 1933 The flow past circular cylinders at low speeds. *Proc. Roy. Soc.* A **141**, 651–669.

TOMOTIKA, S. & AOI, T. 1950 The steady flow of viscous fluid past a sphere and circular cylinder at small Reynolds numbers. *Quart. J. Mech. Appl. Math.* **3**, 140–161.

TRITTON, D. J. 1959 Experiments on the flow past a circular cylinder at low Reynolds numbers. *J. Fluid Mech.* **6**, 547–567.

UNDERWOOD, R. L. 1968 The viscous incompressible flow past a circular cylinder at moderate Reynolds numbers. Ph.D. Dissertation, Stanford University (also SUDAAR Rep. no. 349, AFOSR-68-1664).

VAN DYKE, M. D. 1964*a* The circle at low Reynolds number as a test of the method of series truncation. *Proc. 11th. Int. Cong. Appl. Mech., Munich*, 1165–1169.

VAN DYKE, M. D. 1964*b* *Perturbation Methods in Fluid Mechanics*. New York: Academic.

VAN DYKE, M. D. 1965 A method of series truncation applied to some problems in fluid mechanics. Stanford University SUDAER no. 247.

YAMADA, H. 1954 On the slow motion of viscous liquid past a circular cylinder. *Rep. Res. Inst. Appl. Mech., Kyushu Univ.* **3**, 11–23.